

Generation of microdischarges in diamond substrates

This article has been downloaded from IOPscience. Please scroll down to see the full text article.

2012 Plasma Sources Sci. Technol. 21 022001

(<http://iopscience.iop.org/0963-0252/21/2/022001>)

View [the table of contents for this issue](#), or go to the [journal homepage](#) for more

Download details:

IP Address: 137.222.43.33

The article was downloaded on 06/03/2012 at 11:18

Please note that [terms and conditions apply](#).

FAST TRACK COMMUNICATION

Generation of microdischarges in diamond substrates

S Mitea¹, M Zeleznik², M D Bowden¹, P W May², N A Fox², J N Hart²,
C Fowler³, R Stevens^{3,4} and N StJ Braithwaite¹

¹ Department of Physical Sciences, The Open University, Milton Keynes MK7 6AA, UK

² School of Chemistry, University of Bristol, Bristol BS8 1TS, UK

³ Micro- and Nano-Technology Centre, STFC Rutherford Appleton Laboratory, Didcot OX11 0QX, UK

⁴ School of Science and Technology, Nottingham Trent University, Nottingham NG1 4BU, UK

E-mail: m.bowden@open.ac.uk

Received 4 January 2012, in final form 14 February 2012

Published 1 March 2012

Online at stacks.iop.org/PSST/21/022001

Abstract

We report the generation of microdischarges in devices composed of microcrystalline diamond. Discharges were generated in device structures with microhollow cathode discharge geometries. One structure consisted of an insulating diamond wafer coated with boron-doped diamond layers on both sides. A second structure consisted of an insulating diamond wafer coated with metal layers on both sides. In each case, a single sub-millimetre hole was machined through the conductor–insulator–conductor structure. The discharges were generated in a helium atmosphere. Breakdown voltages were around 500 V and discharge currents in the range 0.1–2.5 mA were maintained by a sustaining dc voltage of 300 V.

(Some figures may appear in colour only in the online journal)

1. Introduction

Research into microdischarges, defined as discharges in which at least one dimension is less than 1 mm, has expanded considerably in recent years and the last decade has seen these devices developed for many different applications [1, 2]. Recent research has seen the investigation of different operating modes, with some authors focusing on device scaling, especially ignition processes [3, 4], while others have investigated operating regimes associated with reproducible instabilities [5–8]. Much of this research has focused on the gas-phase processes that occur in the micro-volumes inside these devices but the role of the surface processes and plasma–surface interactions is gaining increasing attention [9].

Most microdischarge devices reported in the literature consist of metal electrodes separated by an insulating ceramic such as aluminium oxide. A notable exception is the work of Eden *et al* [10, 11], who developed microdischarge arrays based on silicon, produced using technology developed for microelectronics and integrated circuit fabrication. Full understanding of microdischarge physics, including ignition and instability behaviour, requires operation of devices

consisting of a wider range of materials. This is particularly important for small dimension devices, in which the surface area to volume ratio becomes correspondingly large. Although there has been some effort to investigate material influences in microscale devices that operate in pre-breakdown non-self-sustaining modes [12, 13], most development of stable glow-like microdischarges has focused only on a small range of materials.

The thermal, electrical and mechanical properties of diamond make it an attractive material for fabrication of micrometre-size discharge devices. First, the high thermal conductivity of diamond should enable the high gas temperatures generated in microdischarges to be effectively conducted away from the surfaces in contact with the plasma. Second, diamond in its undoped form is an excellent insulator, while doped forms of diamond can be used as electrically conducting layers. This opens up the possibility of all-diamond structures that can be fabricated as a single integrated structure, with the additional advantage that the different layers have well-matched thermal expansion. Third, the hardness and relative inertness of diamond surfaces may enable development of devices that are resistant to

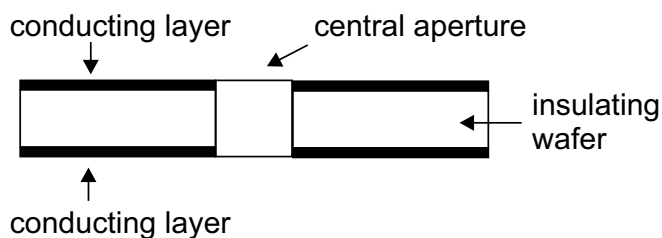


Figure 1. Schematic diagram showing the geometry used for both devices.

thermal and electrical degradation by prolonged exposure to microdischarge plasmas. This could lead to devices with extremely long lifetimes. Finally, the properties of the diamond surfaces, such as the secondary electron emission yield, can be varied by changing the fabrication process [14, 15]. This should enable the effect of surface properties on discharge operation to be systematically investigated. The aim of the research reported here is to demonstrate diamond-based microdischarge devices so that these aspects of microdischarge operation can be studied and new applications explored.

In this communication, we report successful fabrication and operation of microhollow cathode discharge devices based on microcrystalline diamond. Discharges were generated in two devices with similar geometries but different material combinations. In one device, metal electrodes were deposited onto the faces of an undoped microcrystalline diamond wafer. In a second device, the metal electrodes were replaced by layers of p-type microcrystalline diamond, heavily doped with boron, deposited by chemical vapour deposition (CVD).

Figure 1 shows the structure and geometry of the devices. Each device is based on an undoped mechanical-grade polycrystalline CVD diamond freestanding wafer purchased from Element Six (product code: 145-500-0015), polished on one side. The wafer dimensions are $250\ \mu\text{m} \times 10\ \text{mm} \times 10\ \text{mm}$. This was cleaned in warm concentrated nitric acid to remove any residues remaining on the surface after the polishing process.

The metal–diamond–metal device was fabricated using the following process. The wafer was first subjected to a dehydration bake of 30 min on a hot plate, after which layers of titanium (100 nm) and gold (500 nm) were deposited in an SVS E-Gun evaporator. The edges of the wafer were protected with kapton adhesive tape so that a non-conducting border remained between the metal coating and the wafer edge. After coating, the metal layers were annealed using a rapid thermal annealing oven (500°C oven for 2 minutes). A circular hole with $200\ \mu\text{m}$ diameter was then drilled through the centre of the wafer using a micro-machining system (Micronanics Ltd) based on a 355 nm diode-pumped solid-state laser. Finally, the sample was cleaned in an oxygen plasma (PVA TePla America Inc.) for 60 minutes. The purpose of this final step was to remove from the surfaces graphitization that might have been produced by the laser machining process along with any other contamination.

The all-diamond device was based on the same insulating diamond wafer, and produced using the following process. A hot-filament CVD process was used to deposit

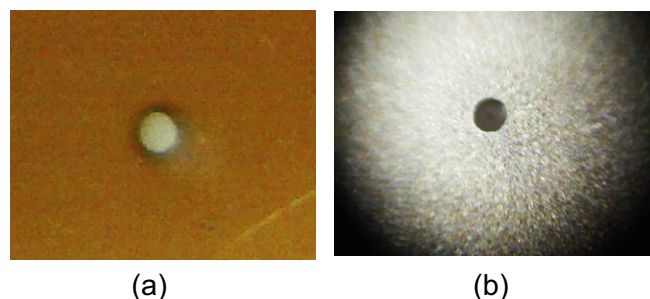


Figure 2. Magnified images of the machined holes for the cases of (a) the device with metal electrodes, showing the $200\ \mu\text{m}$ hole, and (b) the device with conducting diamond electrodes, showing the $300\ \mu\text{m}$ hole.

a layer of heavily boron-doped microcrystalline diamond, approximately $5\ \mu\text{m}$ thick, on either side of this substrate in two sequential steps using standard conditions as described in [14] (Re filament, process pressure 2.6 kPa (20 Torr), 1% CH_4/H_2). B_2H_6 was added to the gas mixture and used as the dopant source at flow rates sufficient to deposit B-doped diamond layers having near-metallic conductivity, with estimated B concentrations of $3 \times 10^{27}\ \text{m}^{-3}$ based on previously calibrated SIMS analysis [16].

A Nd : YAG laser-based micro-machining system (Alpha, Oxford Lasers, UK) was used to drill a $300\ \mu\text{m}$ -diameter hole through the centre of the sample to produce the microplasma cavity. 1 mm was also laser trimmed from each edge of the sample to ensure there was no electrical short-circuit between the upper and lower B-doped layers from unintentional B contamination of the edges. Lastly, the sample was cleaned in hot ($\sim 80^\circ\text{C}$) 90% sulfuric acid + potassium nitrate (2 g in 40 ml of acid) for 15 minutes. This removed any contamination along with any surface graphitization resulting from the laser etching, and left the diamond surfaces oxygen terminated.

Figure 2 shows images of the two devices, obtained using a digital microscope. It can be seen that although the metal layer is slightly discoloured at the edges of the hole, the laser machining process has produced neat circular apertures for both devices.

For each device, plasma ignition was investigated using a chamber back-filled with high-purity helium gas after evacuation to $<1\ \text{Pa}$. Electrical contact was achieved by mechanically pressing tantalum foil strips to each surface. These foil strips were, in turn, connected to the output of a dc high-voltage power supply outside the chamber. A $136\ \text{k}\Omega$ ballast resistor was placed in series with one electrode. Electrical measurements were made using high-voltage probes while photographic images were obtained using a digital microscope.

Figure 3 shows images of the plasma generated using the device with metal electrodes, obtained when the gas pressure was 10 kPa ($\sim 75\ \text{Torr}$). The two images show the plasma for different values of discharge current. Figure 3(a) shows the discharge in a very low-current mode with the plasma confined to the centre of the hole, while figure 3(b) shows the plasma generated for a much higher current, where the plasma has expanded outside the hole over the electrode surface. In both images, the anode side of the discharge is shown.

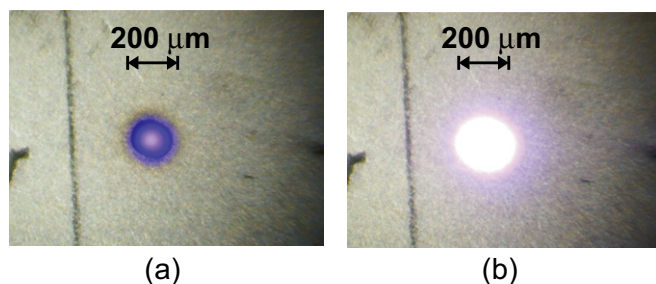


Figure 3. Images of discharges generated by the device with metal electrodes for case of (a) $V = 420$ V, $I = 0.02$ mA and (b) $V = 590$ V, $I = 0.60$ mA. The background gas was helium at a pressure of 10 kPa.

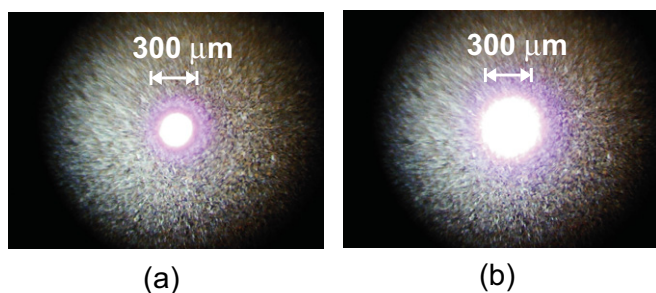


Figure 4. (a) Anode view and (b) cathode view of a discharge generated by the device with semiconducting diamond electrodes, for the case of $V = 410$ V, $I = 0.40$ mA. The background gas was helium at a pressure of 10 kPa.

Figure 4 shows images of the plasma obtained using the device with semiconducting diamond electrodes when the device was operated in a helium atmosphere at 10 kPa (~ 75 Torr). The two images show anode and cathode views of the device being operated under the same conditions. It can be seen that while the discharge is centred in the hole, the plasma on the cathode side of the device spills out over the electrode surface to a much greater extent than for the anode side. This behaviour is consistent with observations reported for comparable microdischarges in devices based on alumina and mica insulators [1–5] and is due to the plasma region expanding over the cathode while the discharge is in a normal glow regime. Similar behaviour was observed for the device with metal electrodes.

Figure 5 shows current–voltage (I – V) curves measured for both devices, obtained for a range of pressures. Each set of data plotted in figure 5 was obtained as the applied voltage was increased and show that, upon ignition, the discharge in each device jumps to a particular value of current. This current then increases as further voltage is applied. Further measurements, not shown, indicate that the minimum breakdown voltage for both devices occurs for values of $pd \sim 5$ Torr cm, where p is the gas pressure and d the electrode separation. Both the shape of the I – V curves and the pd minimum are typical for microhollow cathode discharges.

A detailed comparison of the discharge behaviour is difficult at this stage because the devices have quite different electrical characteristics, even before the discharge is ignited. For the device with metal electrodes, the electrical connection from the power supply to the electrode surface is a simple metal–metal contact, and hence has a constant negligible

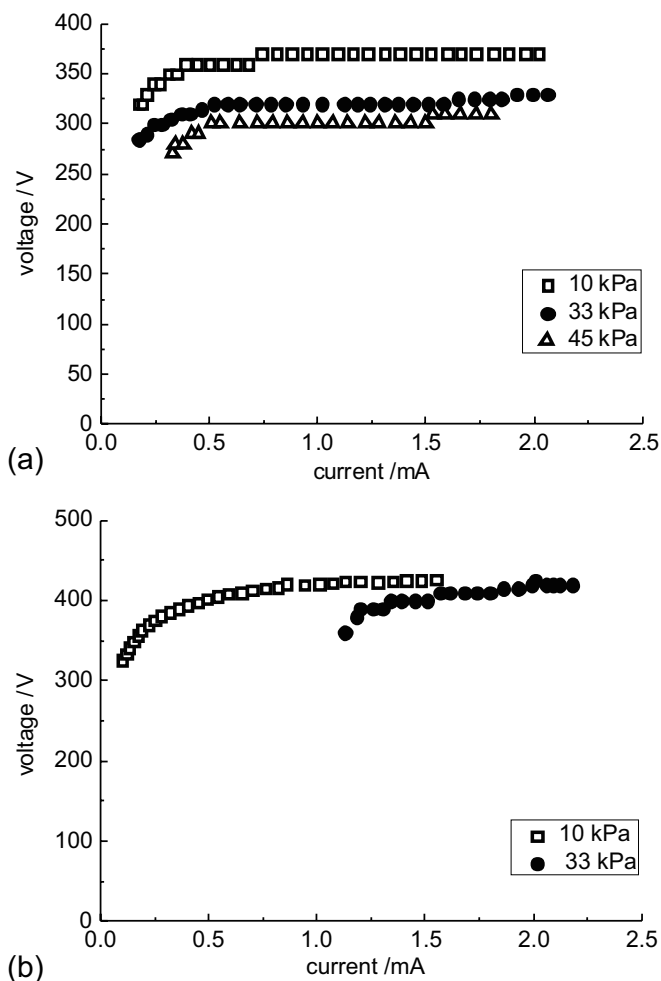


Figure 5. I – V curves obtained at different pressures for (a) the device with metal electrodes and (b) the device with conducting diamond electrodes. Each curve was obtained for increasing applied voltage.

impedance compared with that of the ballast resistor and the discharge itself. For the all-diamond device, however, the electrical contacts to each diamond surface are metal–semiconductor ones and the impedance of these cannot be neglected [17]. Additionally, there will be resistance between the contact and the aperture where the discharge is located. Both the nature of the contact and the conductivity of the conducting diamond layer depend on temperature and hence are difficult to estimate in a simple way. These features will be studied and characterized in a subsequent study. It is clear, however, that the I – V curves shown in figure 5 are consistent with those observed in other studies and indicate that stable, reproducible microdischarges can be generated in these diamond-based structures.

Finally, although we have operated these devices for a relatively short period of time, we can state that each has been operated for more than 5 h without failure. This relatively long lifetime indicates that we can expect these and similar devices to be suitable for more detailed studies of the influence on discharge properties of different material surfaces. It is also promising for potential applications.

The successful operation of diamond-based microdischarge devices represents a new technology for

microdischarge fabrication. Although it was not possible to draw firm conclusions about the effect of the diamond material on the characteristics of the observed microdischarges, it is still possible to conclude that both devices generate microdischarges typical of those observed in microhollow cathode discharges with similar geometry. This demonstration of microdischarges in diamond-based devices offers the opportunity for detailed investigation of the role of material properties in the behaviour of microdischarges. The new technology also has the potential to enable development of a new generation of long-lifetime microdischarge devices.

Acknowledgments

This research is supported by the UK Engineering and Physical Sciences Research Council (EPSRC), under grant EP/G057176/1. The authors are grateful for technical assistance from Sandra Mills, Martin Percy and Fraser Robertson (The Open University), James Smith (University of Bristol) and Adnan Malik and Micronanics Ltd (STFC).

References

- [1] Becker K H, Schoenbach K H and Eden J G 2006 *J. Phys. D: Appl. Phys.* **39** R55–70
- [2] Mariotti D and Sankaran R M 2010 *J. Phys. D: Appl. Phys.* **43** 323001
- [3] Greenan J, Mahony C M O, Mariotti D and Maguire P D 2011 *Plasma Sources Sci. Technol.* **20** 025011
- [4] Müller S, D Luggenhölscher and Czarnetzki U 2011 *J. Phys. D: Appl. Phys.* **44** 165202
- [5] Rousseau A and Aubert X 2006 *J. Phys. D: Appl. Phys.* **39** 1619–22
- [6] Aubert X, Bauville G, Guillon J, Lacour B, Peuch V and Rousseau A 2007 *Plasma Sources Sci. Technol.* **16** 23–32
- [7] Möhr S, Du B, Luggenhölscher and Czarnetzki U 2010 *J. Phys. D: Appl. Phys.* **43** 295201
- [8] Lazzaroni C, Chabert P, Rousseau A and Sadeghi N 2010 *Eur. Phys. J. D* **60** 555–63
- [9] Pitchford L C 2011 *6th Int. Workshop on Microplasmas (3–6 April, Paris, France)*
- [10] Park S-J, Eden J G, Chen J and Liu C 2004 *Appl. Phys. Lett.* **85** 4869–71
- [11] Park S-J and Eden J G 2005 *IEEE Trans. Plasma Sci.* **33** 570–1
- [12] Peterson M S, Zhang W, Fisher T S and Garimella S V 2005 *Plasma Sources Sci. Technol.* **14** 654–60
- [13] Go D B, Fisher T S, Garimella S V and V Bahadur 2009 *Plasma Sources Sci. Technol.* **18** 035004
- [14] Shih A, Yater J, Hor C and Abrams R 1997 *Appl. Surf. Sci.* **111** 251–8
- [15] Bandis C and Pate B B 1995 *Phys. Rev. B* **52** 12056–71
- [16] May P W, Ludlow W J, Hannaway M, Heard P J, Smith J A and Rosser K N 2008 *Diamond Relat. Mater.* **17** 105–17
- [17] Alexander M S, Latto M N, May P W, Riley D J and Pastor-Moreno G 2002 *Diamond Relat. Mater.* **12** 1460–2